Appl. Phys. B 72, 901–907 (2001) / Digital Object Identifier (DOI) 10.1007/s003400100591

Applied Physics B
Lasers
and Optics

Collision dynamics of two Bose–Einstein condensates in the presence of Raman coupling

T. Hong*, **T. Shimizu**

Department of Electronics and Computer Science, Science University of Tokyo in Yamaguchi, 1-1-1 Daigaku-dori, Onoda, Yamaguchi 756-0884, Japan

Received: 5 February 2001/Published online: 27 April 2001 –

Abstract. A collision of two-component Bose-Einstein condensates in the presence of Raman coupling is proposed and studied by numerical simulations. Raman transitions are found to be able to reduce collision-produced irregular excitations by forming a time-averaged attractive optical potential. Raman transitions also support a kind of dark soliton pair in two-component Bose-Einstein condensates. Soliton pairs and their remnant single solitons are shown to be controllable by adjusting the initial relative phase between the two colliding condensates or the two-photon detuning of Raman transitions.

PACS: 03.75.Fi; 32.80.Pj

The realization of high-density Bose–Einstein condensates [1] invokes the study of nonlinear dynamics of matter waves and inventions of various optical techniques to manipulate Bose–Einstein condensates as well as constructions of various matter-wave interferometers for precision measurements. Usually, one would like to reduce irregular excitations and preserve the coherent property of high-density Bose–Einstein condensates as much as possible in many manipulating processes. However, due to the interactions between atoms, the strong repulsive interactions between Bose–Einstein condensates often lead to irregular excitations, especially in collision processes. Inventing a convenient optical technique, which can reduce irregular excitations as well as exert effective control over the Bose–Einstein condensates, is very important.

Raman coupling is a very successful experimental technique for manipulating ultra-cold atomic gas between different internal and external states, because it has the merit of avoiding spontaneous emission loss of atoms in transition processes. For example, recently several experiments have successfully employed Raman coupling in manipulating Bose–Einstein condensates [2].

Here, by proposing a Raman coupling scheme of atomic Bose–Einstein condensates, we show that Raman coupling can also be used to reduce irregular excitations produced in a collision process of two Bose–Einstein condensates. Instead of irregular excitations, the Raman coupling produces a new type of coherent texture, namely, dark soliton pairs in the collision process. Additionally, we also find that these dark soliton pairs and their remnant dark solitons are very sensitive to the initial relative phase between Bose–Einstein condensates and the two-photon detuning of Raman transitions.

The paper is organized as follows: In Sect. 1, we introduce the proposed collision process of two Bose–Einstein condensates in the presence of Raman coupling and the two coupled Gross-Pitaevskii equations for the description of this collision process. In Sect. 2, first we make some simplifications, then we show numerical simulations of the collision process, analyze the function of Raman coupling in the collision process, and discuss the physical origin and some special properties of dark soliton pairs. In Sect. 3, we draw conclusions as well as point out some potential applications of the proposed collision process.

1 Theoretical model

First, we introduce the model in detail by using a schematic, shown in Fig. 1. The black frame in Fig. 1a represents a transverse confining potential $V_0(x, y)$ for two atomic Bose–Einstein condensates 1 and 2 in the abstractively. This potential can be formed, for example, by a blue-detuned hollow laser beam propagating along the z-axis, which has already been demonstrated to be very effective in a recent experiment [3]. Additionally, there are two red-detuned Gaussian laser beams 1 and 2 propagating along x-axis. The intensities of two laser beams are uniform in the x- and y-directions, but of a Gaussian shape in the z-direction, as indicated by the gray levels. Their frequencies are ω_1 and ω_2 respectively, as shown in Fig. 1b. As for the condensates, we assume that atoms have three internal states, $|g_1\rangle$, $|g_2\rangle$ and $|e\rangle$. Thus the two laser beams couple them together and form two Rabi transitions, as shown in Fig. 1b. Because of the negative detuning ($\Delta < 0$) and nonuniform intensities of the two laser beams, they can form two z-axial confining potentials for con-

*Corresponding author.
(Fax: +81-836/88-4543, E-mail: taohong01@163.net)

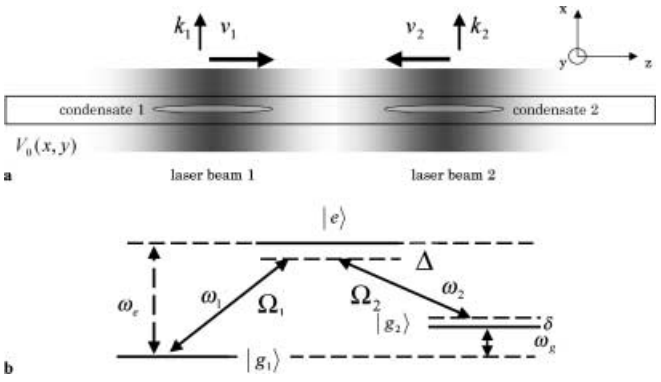

Fig. 1. a Collision and Raman coupling scheme of two atomic Bose–Einstein condensates. **b** Atomic internal energy levels of Bose–Einstein condensates and light coupling. $|g_1\rangle$, $|g_2\rangle$ denote two ground states and $|e\rangle$ denotes an excited state, energy eigenvalues of which are 0, $\hbar\omega_g$ and $\hbar\omega_e$ respectively. The laser beams 1 and 2, with frequencies ω_1 and ω_2 respectively, couple these states together, forming so-called 'Λ' configuration Raman transitions. Ω_1 and Ω_2 are corresponding single-photon Rabi frequencies. The intermediate detuning and two-photon detuning of Raman transitions are $\Delta = \omega_1 - \omega_e$ and $\delta = \omega_1 - \omega_2 - \omega_g$ respectively. Direct transitions between $|g_1\rangle$ and $|g_2\rangle$ are electric-dipole forbidden

densates 1 and 2, which are assumed to be initially distributed in states $|g_1\rangle$ and $|g_2\rangle$, respectively. Additionally, we assume that laser beams 1 and 2 are initially separated by a distance and moving at velocities v_1 and v_2, respectively, in opposite directions. Thus the two condensates are trapped by the two laser beams and moving at velocities the same as those of the laser beams in opposite directions. While the two laser beams overlap, the condensates in the overlap region are transferred between states $|g_1\rangle$ and $|g_2\rangle$ due to the occurrence of Raman transitions. As the two condensates come very close to one another, they collide and interfere with each other.

Next, we derive the equation for the description of this model. As shown in Fig. 1b, because atoms have three internal states, first we generally consider a condensate consisting of three components. To avoid spontaneous emission in a Raman-transition process, we assume that the intermediate detuning Δ of laser beams 1 and 2 is much larger than other characteristic frequencies, such as the natural line width of the atomic transitions and the two-photon detuning δ. As a result, the evolution of the $|e\rangle$-state component adiabatically follows the $|g_1\rangle$- and $|g_2\rangle$-state components, i.e., $\Psi_e = -\left(\Omega_1 \mathrm{e}^{-\mathrm{i}\omega_1 t}\Psi_{g1} + \Omega_2 \mathrm{e}^{-\mathrm{i}\omega_2 t}\Psi_{g2}\right)/(2\Delta)$, where Ψ_e,Ψ_{g1} and Ψ_{g2} are the macroscopic wave functions of the three-component Bose–Einstein condensate in states $|e\rangle$, $|g_1\rangle$ and $|g_2\rangle$ respectively. Then, at zero temperature and under a rotating-wave approximation, the light-coupled $|g_1\rangle$- and $|g_2\rangle$-state components can be described by the following coupled Gross-Pitaevskii equations:

$$\mathrm{i}\hbar\frac{\partial\Psi_{g1}}{\partial t} = -\frac{\hbar^2}{2m}\nabla^2\Psi_{g1} + V_0(x,y)\Psi_{g1} + V_{g1}(z,t)\Psi_{g1} + U_0|\Psi_{g1}|^2\Psi_{g1} + U_0|\Psi_{g2}|^2\Psi_{g1} + \hbar R(z,t)\Psi_{g2}\,, \quad (1)$$

$$\mathrm{i}\hbar\frac{\partial\Psi_{g2}}{\partial t} = -\frac{\hbar^2}{2m}\nabla^2\Psi_{g2} + \hbar\omega_g\Psi_{g2} + V_0(x,y)\Psi_{g2} + V_{g2}(z,t)\Psi_{g2} + U_0|\Psi_{g2}|^2\Psi_{g2} + U_0|\Psi_{g1}|^2\Psi_{g2} + \hbar R^*(z,t)\mathrm{e}^{\mathrm{i}(\omega_2-\omega_1)t}\Psi_{g1}\,, \quad (2)$$

where m is the atomic mass. U_0 describes the atomic interaction strength, which is related to the s-wave scattering length a_{sc} by $U_0 = 4\pi\hbar^2 a_{\mathrm{sc}}/m$. Here we assume that $a_{sc} > 0$, and it is same for all collisions between atoms in the same or different internal states. $V_0(x, y)$ denotes the transverse confining potential, which is common for both $|g_1\rangle$- and $|g_2\rangle$-state components. $V_{g1}(z,t) = \hbar|\Omega_1(\boldsymbol{r},t)|^2/(4\Delta)$ and $V_{g2}(z,t) = \hbar|\Omega_2(\boldsymbol{r},t)|^2/(4\Delta)$ are two localized optical potentials produced by laser beams 1 and 2, respectively. Note that here we assume that the potential V_{g1} (or V_{g2}) can only trap the $|g_1\rangle$-state (or $|g_2\rangle$-state) component even when the two components mix together in the collision process. [1] $R(z,t) = \Omega_1^*(\boldsymbol{r},t)\Omega_2(\boldsymbol{r},t)/(4\Delta)$ is the effective Rabi frequency of two-photon transitions. Because the laser beams 1 and 2 are in Gaussian shape and moving along z-axis, their corresponding Rabi frequencies can be written as $\Omega_1(\boldsymbol{r},t) = \Omega_{10}\mathrm{e}^{-(z-z_{01}-v_1t)^2/a_1^2}\mathrm{e}^{-\mathrm{i}\boldsymbol{k}_1\cdot\boldsymbol{r}}$ and $\Omega_2(\boldsymbol{r},t) = \Omega_{20}\mathrm{e}^{-(z-z_{02}-v_2t)^2/a_2^2}\mathrm{e}^{-\mathrm{i}\boldsymbol{k}_2\cdot\boldsymbol{r}}$, where Ω_{10} and Ω_{20} are maximum magnitudes of the two Rabi frequencies, z_{01} and z_{02} are initial center positions, a_1 and a_2 are half widths, and $\boldsymbol{k}_1$ and $\boldsymbol{k}_2$ are wavevectors of the two laser beams, respectively. Additionally, we assume that the wavevectors $\boldsymbol{k}_1$ and $\boldsymbol{k}_2$ are approximately equal, then the two-photon Rabi frequency can be written as $R(z,t) = \Omega_{10}\Omega_{20}\mathrm{e}^{-(z-z_{01}-v_1t)^2/a_1^2-(z-z_{02}-v_2t)^2/a_2^2}/(4\Delta)$. It is evident that when and only when the two potentials $V_{g1}(z,t)$ and $V_{g2}(z,t)$ overlap with each other does the effective two-photon Rabi frequency becomes finite. Thus the description of the Bose–Einstein condensate has now been reduced from three components to two components.

2 Numerical simulation

For simplicity and to give more importance to the analysis of the affect of Raman transitions on the collision, we need to make some simplifications. We assume the transverse confining potential $V_0(x, y)$ to be so tight and the z-axial confining potentials $V_{g1}(z,t)$ and $V_{g2}(z,t)$ to be so loose that in the description of the transverse modes of the Bose–Einstein condensate we can neglect the affect of $V_{g1}(z,t)$ and $V_{g2}(z,t)$ as well as interactions between atoms. We assume that in the description of the longitudinal modes the longitudinal dimension of the condensate is much larger than the healing length. We assume that the transverse dimensions of the condensate are very small and the time scale for adjustment of the transverse profile of the condensate to the equilibrium form appropriate for the instantaneous number of atoms per unit length is small compared with the time for

[1] In experiments, we think there are two methods to realize a trapping of two components respectively by two laser beams. One method is to assume that the energy difference of the two internal ground states $\hbar\omega_g \gg \hbar\Delta$. Thus one laser beam is only effective for one of the components and has little effect on the other component, due to the detuning of the single-photon transition of the other component being very large. The other way is to assume that the internal states are some proper magnetic sublevels and laser beams are polarized. For example, two ground states $|g_1\rangle$ and $|g_2\rangle$ are $|+1\rangle$ and $|-1\rangle$, respectively; the excited state $|e\rangle$ is $|0\rangle$; and the polarizations of two laser beams are $\sigma+$ and $\sigma-$, respectively. Thus the $\sigma+$-polarized (or $\sigma-$-polarized) laser beam can only couple two states $|-1\rangle$ and $|0\rangle$ (or $|+1\rangle$ and $|0\rangle$). As a result, the potential, produced by one laser beam, can only trap one component.

an excited pulse to pass a given point. This is a low-density approximation, in fact, similar to that used in [4]. Thus, by letting $\Psi_{g1}(\boldsymbol{r}, t) = f_{g1}(z, t)g_{g1}(x, y)\mathrm{e}^{-\mathrm{i}\mu_1 t/\hbar}$ and $\Psi_{g2}(\boldsymbol{r}, t) = f_{g2}(z, t)g_{g2}(x, y)\mathrm{e}^{-\mathrm{i}\mu_2 t/\hbar}$ and through a deduction similar to that in [4], we can obtain simplified one-dimensional Gross-Pitaevskii equations:

$$\mathrm{i}\hbar\frac{\partial f_{g1}}{\partial t} = -\frac{\hbar^2}{2m}\frac{\partial^2 f_{g1}}{\partial z^2} + V_{g1}(z, t)\, f_{g1} + U_0^{'}|f_{g1}|^2 f_{g1} + U_0^{''}|f_{g2}|^2 f_{g1} + \hbar R(z, t)\mathrm{e}^{-\mathrm{i}(\mu_2-\mu_1)t/\hbar} f_{g2} \tag{3}$$

$$\mathrm{i}\hbar\frac{\partial f_{g2}}{\partial t} = -\frac{\hbar^2}{2m}\frac{\partial^2 f_{g2}}{\partial z^2} + \hbar\omega_g f_{g2} + V_{g2}(z, t)\, f_{g2} + U_0^{'}|f_{g2}|^2 f_{g2} + U_0^{''}|f_{g1}|^2 f_{g2} + \hbar R^*(z, t)\mathrm{e}^{\mathrm{i}(\omega_2-\omega_1)t+\mathrm{i}(\mu_2-\mu_1)t/\hbar} f_{g1}, \tag{4}$$

where g_{g1} and g_{g2} are the normalized transverse modes of the two components, μ_1 and μ_2 are the chemical potentials of g_{g1} and g_{g2} respectively, f_{g1} and f_{g2} are the longitudinal wave functions, $U_0^{'} = U_0 \int |g_{g1}(x, y)|^4 \mathrm{d}x\mathrm{d}y$ and $U_0^{''} = U_0 \int |g_{g1}(x, y)g_{g2}(x, y)|^2 \mathrm{d}x\mathrm{d}y$.

As an initial condition for the collision process, we assume that the two-component Bose–Einstein condensate is initially separated into two condensates, i.e., $\Psi_{g1}(\boldsymbol{r}, t)|_{t=0}$ and $\Psi_{g2}(\boldsymbol{r}, t)|_{t=0}$, which are trapped in the ground states of the two moving potentials, $V_{g1}(z, t)$ and $V_{g2}(z, t)$, respectively. For simplicity, we assume that the two potentials have the same shapes, depths and speeds (but in opposite directions); thus the transverse and longitudinal modes of the two initial ground-state Bose–Einstein condensates are the same shape, and the condensates have same numbers of atoms and the same chemical potentials.

We use the split operator method to solve the above time-dependent Gross-Pitaevskii equations, 3 and 4. First, we show a typical collision process in the presence of Raman coupling in Figs. 2a,b and 3. For comparison, in Fig. 2c and d, we also show another collision in which two condensates the same as the above are trapped by two potentials similar to $V_{g1}(z, t)$ and $V_{g2}(z, t)$, but there are no Raman transitions between them. The elimination of Raman transitions is possible so long as the two laser beams couple the two ground states $|g_1\rangle$ and $|g_2\rangle$ with different excited states instead of one common excited state. The parameter values used in the numerical simulation are $\Omega_{10}^2/(4\Delta) = \Omega_{20}^2/(4\Delta) = \Omega_{10}\Omega_{20}/(4\Delta) = -6000/\tau$, $v_1 = -v_2 = 9a_1/\tau$, $a_2 = a_1$, $U_0^{'} = U_0^{''} = 2000\hbar/\tau$, $z_{01} = -z_{02} = -a_1$, and the chemical potentials of initial ground-state Bose–Einstein condensates are both $\mu_0 = -3.99 \times 10^3\hbar/\tau$, where

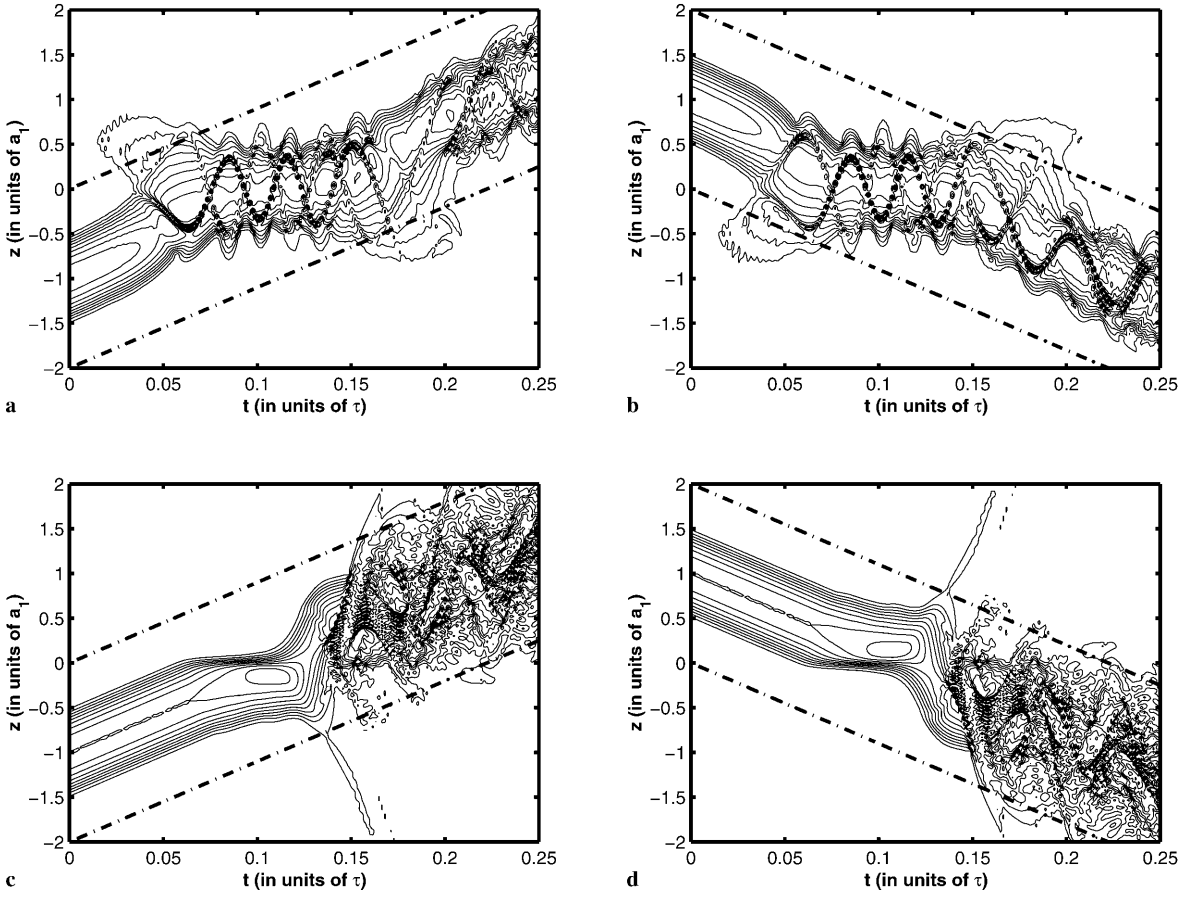

Fig. 2a–d. Contour plots of time evolution of the condensate wave functions $|f_{g1}|$ and $|f_{g2}|$ in two collision processes. **a** $|f_{g1}|$ and **b** $|f_{g2}|$ in the collision with Raman coupling. **c** $|f_{g1}|$ and **d** $|f_{g2}|$ in the collision without Raman coupling. In these collisions, the initial phases of f_{g1} and f_{g2} are $\pi/4$ and 0 respectively, and the detuning $\delta = 0$. *Dash-dotted lines* denote the boundaries of the corresponding axial optical potential, $V_{g1}(z, t)$ or $V_{g2}(z, t)$. These boundaries correspond to the boundaries of Gaussian laser beams at the $1/\mathrm{e}$ of maximum intensities. Between $t = 0.05\tau$ and 0.15τ, there are four zigzag density dip traces in Fig. 2a and b. These traces indicate the oscillations of four dark solitons inside the condensates

a_1 and $\tau = 2ma_1^2/\hbar$ are considered as the unit length and the unit time respectively. In choosing these parameter values, we have referred to some experimental results [1, 3, 5]. We think these values are within reasonable range of those experimental results. Here we use fairly large values of the chemical potentials, so that the repulsive interactions within and between two condensates are very strong, to produce nonlinear excitations.

In the collision without Raman transitions, the two condensates obstruct their passing through each other because of repulsive interactions between atoms, as shown in Fig. 2c and d. After the collision, we can see that small parts of condensates radiate out of the axial optical potentials; the remnant Bose–Einstein condensates oscillate violently in the potentials. The violent oscillations appear to be very irregular. In contrast, Figs.2 a,b and 3 show that while Raman transitions exist the radiation becomes very weak; the violent oscillations of remnant Bose–Einstein condensates are much reduced. This indicates that the repulsive interaction between two Bose–Einstein condensates is greatly counteracted by an attractive optical potential produced by Raman transitions. We can understand the formation of this potential in the following way: Because Raman transitions can transfer each condensate between two components, f_{g1} and f_{g2} circularly, each condensate interacts alternatively with the two axial optical potentials V_{g1} and V_{g2}. As a result, the light-shifted energy of each condensate, produced by the two laser beams, becomes a temporal combination of V_{g1} and V_{g2}, and each condensate feels a vibrating optical potential locating at the collision center $z = 0$. According to the overlap form of V_{g1} and V_{g2}, the vibrating potential is on average attractive. Thus this time-averaged attractive potential counteracts the repulsive interaction between the two condensates, so it becomes much easier for them to pass through each other. We therefore observe the oscillation amplitudes of the condensates, produced by the repulsive interaction, to become much small. But between $t = 0.05\tau$ and 0.15τ, we can still observe that the volume of each condensate oscillates slightly in the collision process due to the vibration of the attractive optical potential. In the collision process, we also observe that dark solitons are generated, as shown in Fig. 3. Formations of dark solitons are due to the interference of collision condensates. Although the two condensates are initially distributed in two different internal states, Raman transitions can transfer parts of them from one of the internal states to the other in the collision process. Consequently, when the transferred part of one condensate overlaps with the part of the other condensate in the same internal state, interference fringes are produced. Due

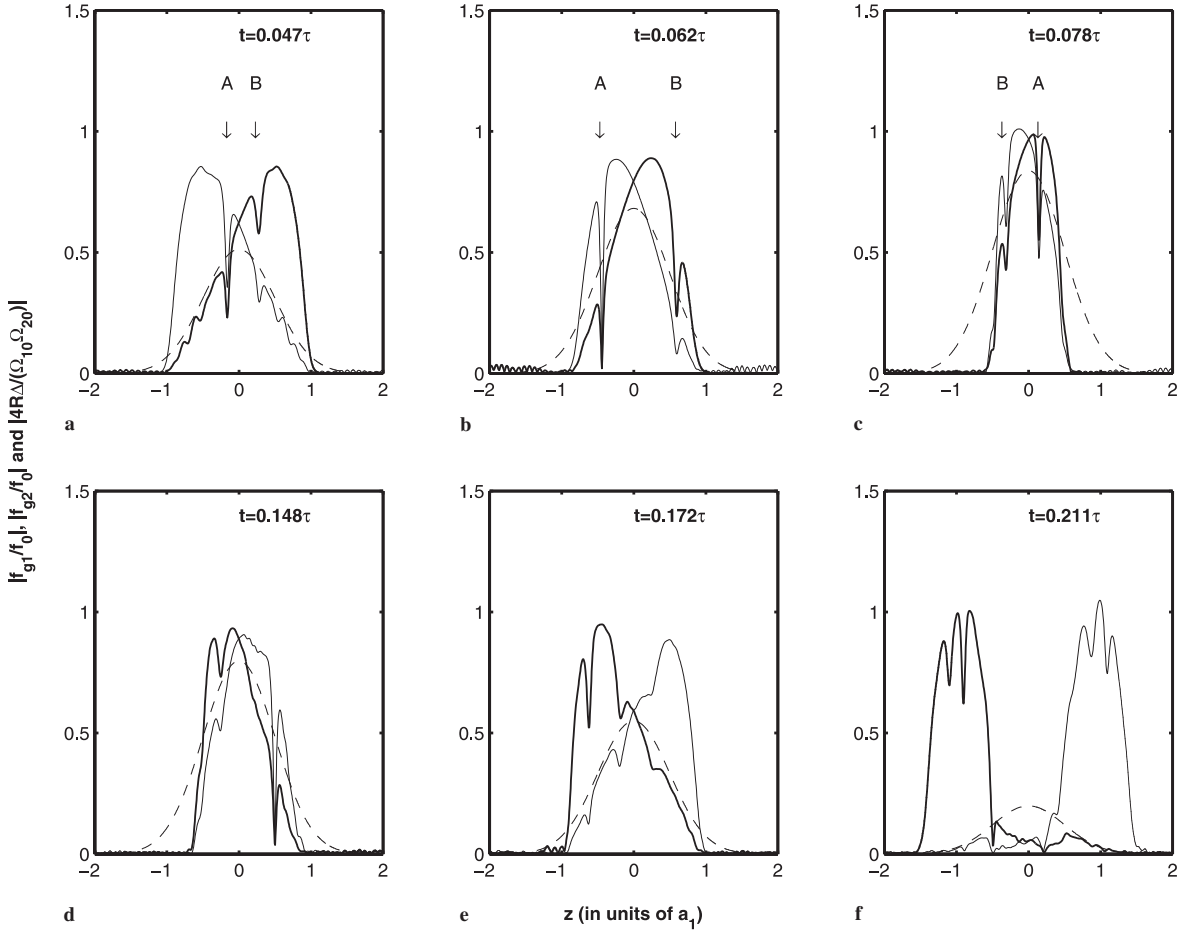

Fig. 3a–f. Generation of dark soliton pairs in the collision with Raman coupling and remnant single solitons. *Thin solid lines* denote $|f_{g1}/f_0|$, *thick solid lines* denote $|f_{g2}/f_0|$ and *dashed lines* denote $|4R\Delta/(\Omega_{10}\Omega_{20})|$. f_0 is the maximum of $|f_{g1}|_{t=0}$ and $|f_{g2}|_{t=0}$. There are four dark solitons in each figure of **a**, **b** and **c**. *Arrow A* marks one soliton pair, and *arrow B* marks another soliton pair. The values of t denote the time of the subfigures sampled from the collision process shown in Fig. 2a and b

to the nonlinear effect of condensates, interference fringes evolve into dark solitons. It is evident that this process is similar to that in [6].

However, solitons produced in this collision process in the presence of Raman coupling are quite different from those single solitons described in [4, 5, 7]. One of the important differences is that these solitons always appear in pairs. As shown in Fig. 3a-d, in the collision process, every soliton in one component of the condensates always has a corresponding soliton in the other component at the same spatial position. Another important difference is that the density difference between the two components does not lead to a speed difference between two solitons in a pair. As shown in Fig. 3a and b, sometimes the two components have quite different local densities at the location of a soliton pair; however, solitons in the pair always move synchronously in the condensates. The reason for the synchronous motion of the two solitons in a pair is that Raman transitions associate the two components tightly and consequently lock their phases together. As we can see in Fig. 4, the phases of two components are almost completely the same in the region of strong Raman transitions, which are indicated by the magnitudes of the normalized two-photon Rabi frequency $|4R\Delta/(\Omega_{10}\Omega_{20})|$. Dark solitons are phase kinks in essence, so there is no doubt that solitons, with similar spatial phases, in a pair move synchronously. Additionally, the cross-phase modulation between dark solitons in a pair also leads to a repulsive effect between them and tends to separate them. It is evident that this repulsive effect is also counteracted by Raman transitions, which produce an equivalently attractive effect between solitons in the pair by locking their phases together. Even after a collision of two soliton pairs, A and B, solitons in each pair can still preserve their waveforms and trajectories well, as shown in Figs. 3b,c and 2a,b respectively. This illustrates that collisions between soliton pairs are elastic collisions, which is usually considered as an important common characteristic of all kinds of solitons. The synchronous motion of solitons in the pair also indicates that the propagation speed of the soliton pair is determined by the total local density of the two components instead of each single component. We can find this property from Fig. 2a,b. The propagation speed of the soliton pair, in the region $z < 0$, at time $t = 0.078\tau$ is larger than that at time $t = 0.047\tau$, because the total density of the two components is increased in the overlap region. Some similarities between a soliton pair and a single soliton can also be seen. For example, the propagation speed, the width and the density contrast of a soliton pair also depend on the value of its phase kink, which is also varied by the local density gradient. We can find these properties by careful observation of Figs. 2a,b, 3 and 4.

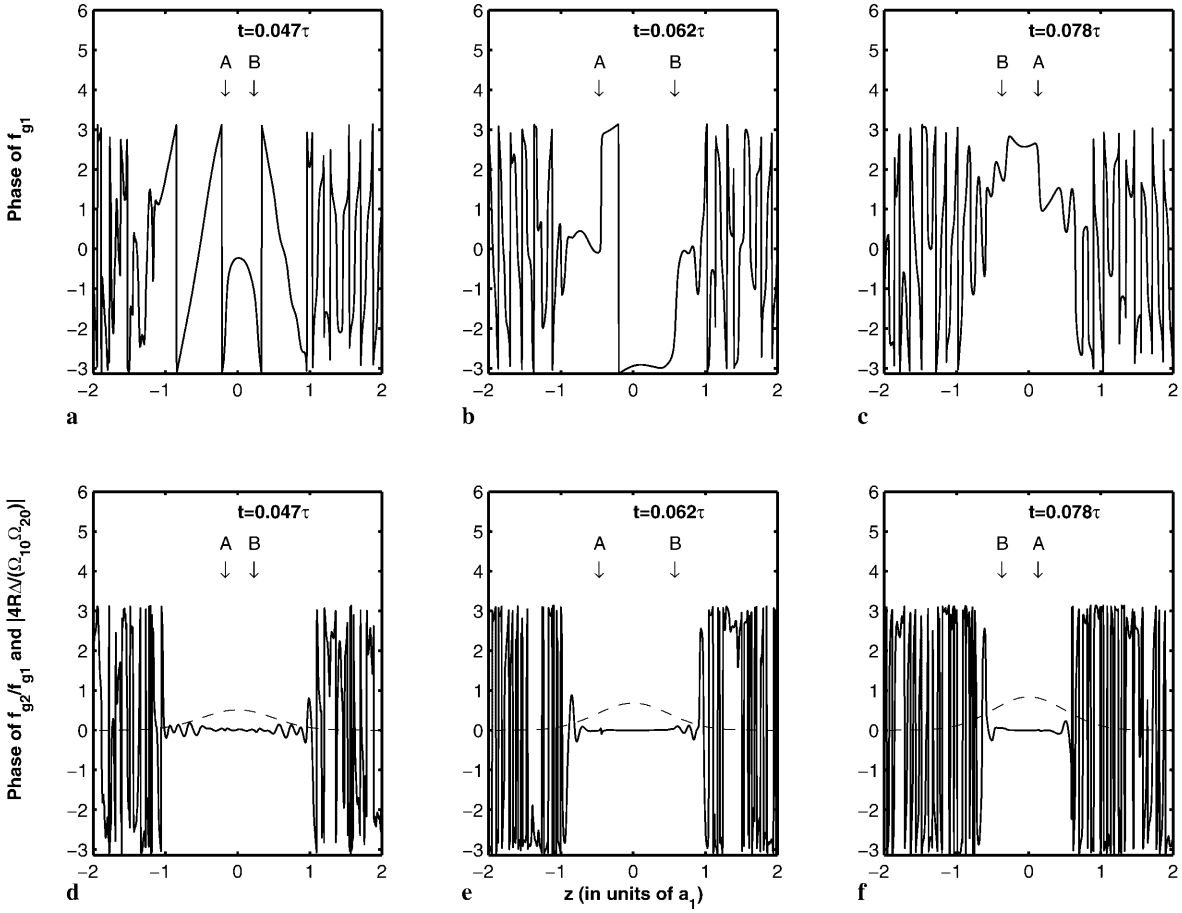

Fig. 4a–f. Phase evolution of the condensate wave functions in the collision with Raman coupling. The *solid lines* in **a**–**c** denote the phase of f_{g1}, the *solid lines* in **d**–**f** denote the phase of f_{g2}/f_{g1}, and the *dashed lines* denote $|4R\Delta/(\Omega_{10}\Omega_{20})|$. *Arrow A* marks the position of one soliton pair, and *arrow B* marks the position of the other dark soliton pair. The values of t denote the time of the subfigures sampled from the collision process shown in Fig. 2a and b

Because the density of the condensates varies in a parabola-like form in space, we find that its phase kink flips in the boundary region of the condensates; simultaneously, its speed flips too, and as a result, the soliton pair oscillates inside the condensates.

The two components of the condensates begin to separate very apparently after $t = 0.15\tau$, because of the separation of the two axial optical potentials, as shown in Fig. 2a,b. Simultaneously, Raman transitions become weaker and weaker because of the decrease in the overlap of the two laser beams, as shown in Fig. 3d–f. As a result, soliton pairs become unstable and are to be separated in this process. Critically depending on the local evolution of the two components, some solitons disappear and some remain and propagate into the separated one-component condensates, as shown in Figs. 2a,b and 3e,f. Because of the disappearance of the cross-phase modulation in each one-component condensate, the oscillation behaviors of the remnant single solitons are different from those of the soliton pairs. Especially the oscillation periods of the remnant single solitons appear to be quite different from those of the previous soliton pairs.

The generation of dark soliton pairs is controllable. Usually, the relative phase between two condensates in different internal states is meaningless because of the orthogonality of the internal states. However, here Raman transitions can form a circulation of atoms between the two internal states; the relative phases between the two condensates are related and therefore becomes very important. Because the formation of dark soliton pairs is due to the interference of colliding condensates, we can also control the generation of soliton pairs as well as remnant single solitons by adjusting the initial relative phase between two colliding condensates or the two-photon detuning of Raman transitions, as shown in Fig. 5.

In the above, we have discussed the collision of two Bose–Einstein condensates under the one-dimensional approximation. However, will a three-dimensional collision be completely different from the one-dimensional collision? Some difference must exist. For example, in a three-dimensional process, dark soliton pairs might be distorted by transverse perturbations and evolve into vortices, because similar behaviors of single dark solitons have been found [5]. However, in the above analysis, we have already found that the function of Raman coupling in the collision process is, in fact, to lock the phases of the two components of the condensates by forming strong atom circulation between the two internal states, and as a result, solitons appear in pairs. As for vortices, they are phase singular points, so they are quite similar to dark solitons in essence. We think that Raman coupling can also lock the phases of two components of the condensates in a three-dimensional case, and vortex pairs might therefore be formed. Certainly, a more affirmative answer should be obtained from a numerical simulation

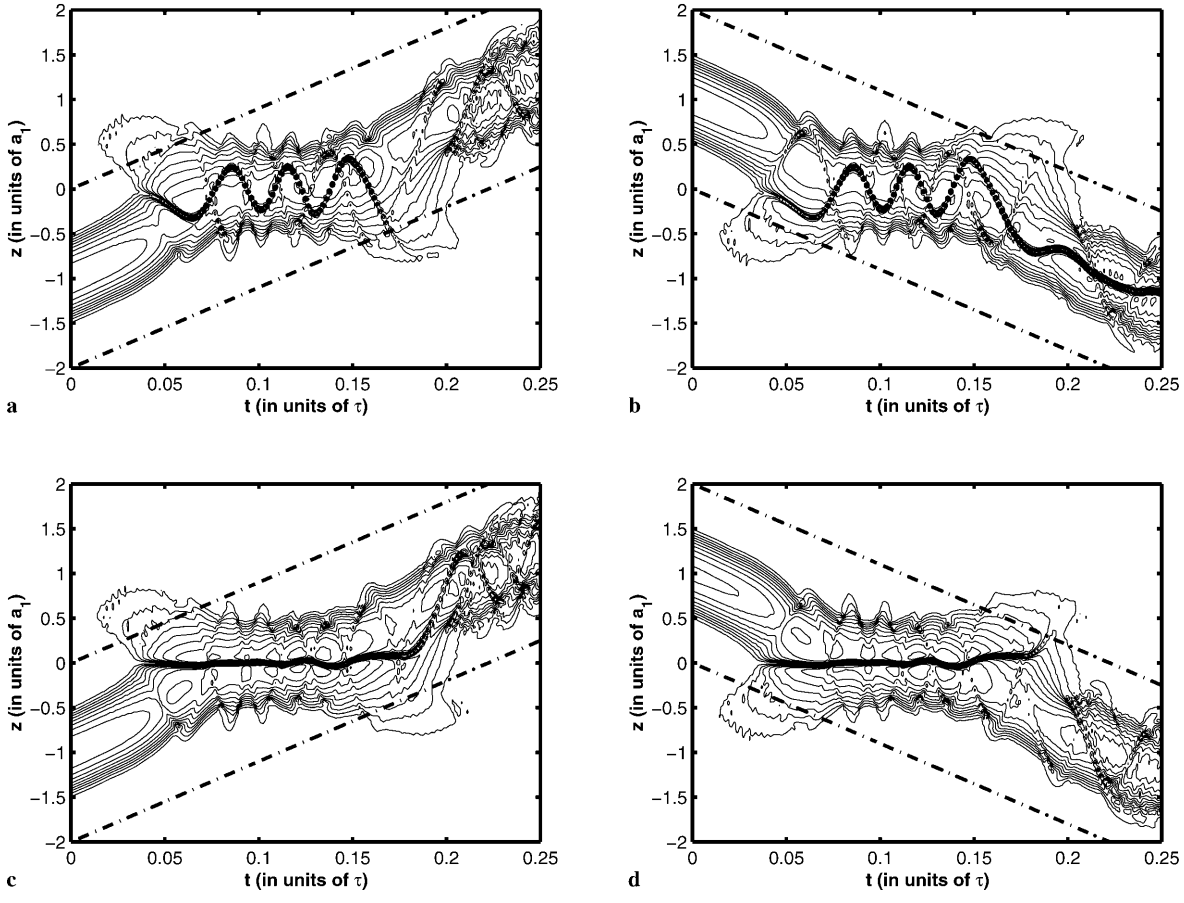

Fig. 5a–d. Contour plots of the time evolution of the condensate wave functions $|f_{g1}|$ and $|f_{g2}|$ in two collision processes. **a** $|f_{g1}|$ and **b** $|f_{g2}|$ in one collision. In this collision, the initial phases of f_{g1} and f_{g2} are $\pi/2$ and 0 respectively, and the detuning $\delta = 0$. **c** $|f_{g1}|$ and **d** $|f_{g2}|$ in the other collision. In this collision, the initial phases of both f_{g1} and f_{g2} are 0, and the detuning $\delta = 100/\tau$. *Dash-dotted lines* denote the boundaries of the corresponding axial optical potential, $V_{g1}(z, t)$ or $V_{g2}(z, t)$. These boundaries correspond to the boundaries of Gaussian laser beams at 1/e of the maximum intensities

of a three-dimensional collision, which will be done in future work.

3 Conclusion

In conclusion, we have proposed a new Raman coupling scheme for Bose–Einstein condensates and analyzed the influence of Raman transitions on the collision and excitation of two-component Bose–Einstein condensates. We have found that Raman transitions can reduce collision-produced irregular excitations by forming a time-averaged attractive potential. Raman transitions also support a new kind of dark soliton, i.e., dark soliton pairs in two-component Bose–Einstein condensates, by locking the phases of the two components. We have also shown the control of soliton pairs and their remnant single solitons by adjusting the initial relative phase between the two colliding condensates and the two-photon detuning of Raman transitions. The dynamical sensitivity of the dark soliton pairs and remnant solitons to these parameters indicates that the proposed collision can be used in the measurement of relative phase between different high-density Bose–Einstein condensates. Currently, constructions of various interferometers with matter waves for high-precision measurements are being considered. We think that this proposal might provide a useful method in this field.

Acknowledgements. T. Hong thanks Japan Science Promotion Society for partial financial support. This work was supported by a Grant-in-Aid for JSPS Fellows from the Ministry of Education, Science, Sports and Culture of Japan.

References

1. M.H. Anderson, J.R. Ensher, M.R. Matthews, C.E. Wieman, E.A. Cornell: Science **269**, 198 (1995); K. Davis, M.-O. Mewes, M.R. Andrews, N.J. van Druten, D.S. Durfee, D.M. Kurn, W. Ketterle: Phys. Rev. Lett. **75**, 3969 (1995); C.C. Bradley, C.A. Sackett, J.J. Tollet, R.G. Hulet: Phys. Rev. Lett. **78**, 985 (1997); D.G. Fried, T.C. Killian, L. Willmann, D. Landhuis, S.C. Moss, D. Kleppner, T.J. Greytak: Phys. Rev. Lett. **81**, 3811 (1998)
2. E.W. Hagley, L. Deng, M. Kozuma, J. Wen, K. Helmerson, S.L. Rolston, W.D. Phillips: Science **283**, 1706 (1999); M.-O. Mewes, M.R. Andrews, D.M. Kurn, D.S. Durfee, C.G. Townsend, W. Ketterle: Phys. Rev. Lett. **78**, 582 (1997); I. Bloch, T.W. Hänsch, T. Esslinger: Phys. Rev. Lett. **82**, 3008 (1998); B.P. Anderson, M.A. Kasevich: Science **282**, 1686 (1998); A.P. Chikkatur, A. Görlitz, D.M. Stamper-Kurn, S. Inouye, S. Gupta, W. Ketterle: Phys. Rev. Lett. **85**, 483 (2000)
3. K. Bongs, S. Burger, S. Dettmer, D. Hellweg, J. Arlt, W. Ertmer, K. Sengstock: e-print cond-mat/0007381
4. A.D. Jackson, G.M. Kavoulakis, C.J. Pethick: Phys. Rev. A **58**, 2417 (1998)
5. M.R. Andrews, D.M. Kurn, H.-J. Miesner, D.S. Durfee, C.G. Townsend, S. Inouye, W. Ketterle: Phys. Rev. Lett. **79**, 553 (1997); S. Burger, K. Bongs, S. Dettmer, W. Ertmer, K. Sengstock, A. Sanpera, G.V. Shlyapnikov, M. Lewenstein: Phys. Rev. Lett., **83**, 5198 (1999); J. Denschlag, J.E. Simsarian, D.L. Feder, C.W. Clark, L.A. Collins, J. Cubizolles, L. Deng, E.W. Hagley, K. Helmerson, W.P. Reinhardt, S.L. Rolston, B.I. Schneider, W.D. Phillips: Science **287**, 97 (2000)
6. T.F. Scott, R.J. Ballagh, K. Burnett: J. Phys. B **31**, L329 (1998)
7. W. Zhang, D.F. Walls, B.C. Sanders: Phys. Rev. Lett. **72**, 60 (1994); T. Hong, Y.Z. Wang, Y.S. Huo: Phys. Rev. A **58**, 3128 (1998); W.P. Reinhardt, C.W. Clark: J. Phys. B **30**, L785 (1997); A.E. Muryshev, H.B. van Linden van den Heuvell, G.V. Shlyapnikov: Phys. Rev. A **60**, R2665 (1999); P.O. Fedichev, A.E. Muryshev, G.V. Shlyapnikov: Phys. Rev. A **60**, 3220 (1999); Th. Busch, J.R. Anglin: Phys. Rev. Lett. **84**, 2298 (2000); L.D. Carr, C.W. Clark, W.P. Reinhardt: Phys. Rev. A **62**, 063610 (2000)